Nonlinear Dynamics and Systems Theory, **24** (3) (2024) 217–227

Improved Power Quality with Active Shunt Power Filter Based on Optimized PI Controller and Flying Squirrel Search MPPT Technique Applied to the WECS

A. Abbadi [1*], F. Hamidia [1], A. Morsli [1], M. R. Skender [2] and A. Tlemçani [1]

[1] *Research Laboratory in Electrical Engineering and Automatic (LREA), University of Medea, Algeria.*

[2] *Renewable Energy and Materials Laboratory (REML), University of Medea, Algeria.*

Received: October 14, 2023; Revised: May 3, 2024

Abstract: This paper aims to improve power quality issues following the IEEE 519 power quality standard recommendations. Indeed, the existing electrical distribution system employs highly nonlinear loads, which raises concerns about the quality of electrical energy. To solve these problems, an optimized PI controller and a bio-inspired MPPT controller are applied to a Wind Energy Conversion System (WECS) integrated with a Shunt Active Power Filter (SAPF). The MPPT controller is used for extracting maximum power from the WECS using the Flying Squirrel Search (FSS) algorithm. In order to overcome the problem of the dynamic performance of DC Link voltage that occurs when using the traditional PI control, an adaptive PI controller using the Sliding Mode Extremum-Seeking (SMES) algorithm is adopted. The SMES algorithm is utilized here to reduce a selected cost function that brings the required performance aspects. The dynamic performance of the SAPF is optimized using the direct power control technique. Simulation results are provided to confirm the effectiveness of the proposed controllers. They clearly demonstrate that the applied control algorithms are effective in eliminating harmonic currents and injecting the available active power of the wind turbine into the load and power grid.

Keywords: *SAPF; THD; WECS; MPPT controller; FSS algorithm; adaptive PI controller; SMES technique.*

Mathematics Subject Classification (2010): 93E11, 93-XX, 93B12, 90C59.

* Corresponding author: mailto:amel.abbadi@yahoo.fr

1 Introduction

With substantial advancements in power electronics and microelectronics technology in recent years, the propagation of nonlinear loads such as static power converters has impaired the power quality in transmission systems energy distribution. Indeed, the current waveform is not purely sinusoidal on the network mainly due to high harmonic currents. This results in a reduced power factor, decreased efficiency, and decreased system performance which is not allowed according to the recommendations of the IEEE 519 power quality standard [1–3].

Using passive LC has always been the simplest way to reduce current harmonics and boost the power factor. However, there are numerous drawbacks to using a passive filter [4, 5]. Because of the rapid advancement of modern power electronic technology, earlier efforts have primarily focused on active filters rather than passive filters. One of the most common active filters is the shunt active power filter (SAPF). It injects currents that are equal and at the same time opposite to the harmonic components, allowing only the fundamental components to flow through the point of common coupling (PCC) [5].

DC-link voltage directly affects the performance of shunt active power filters (SAPFs). Maintaining voltage stability of the DC-link voltage has a direct impact on the system output and is critical to ensuring the converters operate properly. In SAPFs, DC-link voltage regulators are critical for mitigating fluctuations in instantaneous active power [6].

The shunt active power filter is powered by a DC voltage source or a capacitor which is expensive [1]. In our case, we propose another free continuous source, which is the wind energy. The Wind Energy Conservation System (WECS) based on the SAPF is used to improve power quality. It ensures bidirectional energy flow while extracting maximum energy under different wind speeds [4, 5]. As we know, the MPPT controller can extract the maximum energy from the WECS by adjusting the duty cycle of the boost converter. MPPT offers a variety of control strategies, such as perturbation and observation (P&O), fuzzy logic, neural network, etc. [5]. However, there are only a few publications on bio-inspired MPPT techniques for the WECS [7,8]. The most significant advantage of bio-inspired MPPT algorithms is that they do not require mathematical modeling of the process to improve control; their convergence speed is appreciable; and they are robust to load variations [9, 10].

In this paper, two regulators are proposed to ensure the maintenance of the THD of current sources according to the IEEE 519 standard in the SAPF connected to a WECS. The first controller is the flying squirrel search optimization (FSSO) MPPT controller. This MPPT technique is proposed to extract the maximum power from the WECS. The second controller is the DC-link voltage controller based on an adaptive PI controller which uses the sliding-mode extremum-seeking technique to enhance compensation adaptability for fluctuation in wind speed.

This paper is structured as follows. Section 2 describes the system under consideration. Control strategies of a shunt active power filter in a grid-integrated wind system are presented in Section 3. Section 4 employs simulations to assess the efficacy of the proposed controllers. Finally, the conclusions are presented in Section 5.

2 Configuration of the System

The structure of the shunt active power filter connected to the wind energy conversion system (WECS) is presented in Figure 1. In this system, a permanent magnet syn-

chronous generator (PMSG) wind turbine is coupled to the grid and a nonlinear load via a shunt active power filter. The inverter converts power from the wind turbine in addition to compensating for harmonic currents.

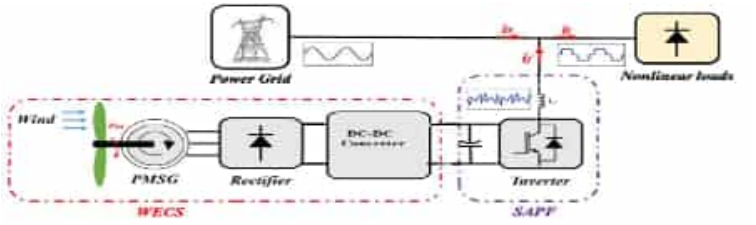

Figure 1: Block Diagram of the SAPF connected to the WECS.

2.1 Wind energy conversion system

As shown in Figure 1, the wind energy conversion system is formed up of a wind turbine that transforms wind energy into mechanical energy. A gearbox connects the wind turbine shaft to the shaft of the permanent magnet synchronous generator. The generator generates nominal three-phase voltages and currents, which are then fed into a three-phase rectifier. The resulting DC signal is amplified in a DC/DC boost converter [7].

2.2 Shunt active power filter

The operation of the SAPF is based on the fact that the harmonic currents are produced equally in amplitude and in phase opposite to these harmonics generated by the nonlinear loads and circulating in the network. As a result, the SAPF current is generated in such a way that the network current's sinusoidal shape is retained. The typical structure of a SAPF includes a converter, a DC-link capacitor and a filter inductor, as illustrated in Figure 1 [1, 3].

3 Control Strategies of Shunt Active Power Filter in Grid-Integrated Wind System

Figure 2 depicts the different control strategies adopted for the integrated wind system with a grid-connected shunt active power filter. In this section, we will describe in detail the MPPT flying squirrel search controller of the WECS and the adaptive PI controller of the DC Link voltage control loop.

3.1 Flying Squirrel Search MPPT controller

3.1.1 Overview of the FSSO algorithm

The search process begins when flying squirrels start looking for food. During the warm season (fall), squirrels glide from one tree to the next in quest of food. They shift their location and explore different regions of the forest while doing so. They can achieve their daily energy requirements more quickly on a diet of abundantly accessible acorns since the climatic conditions are warm enough and hence consume the acorns promptly

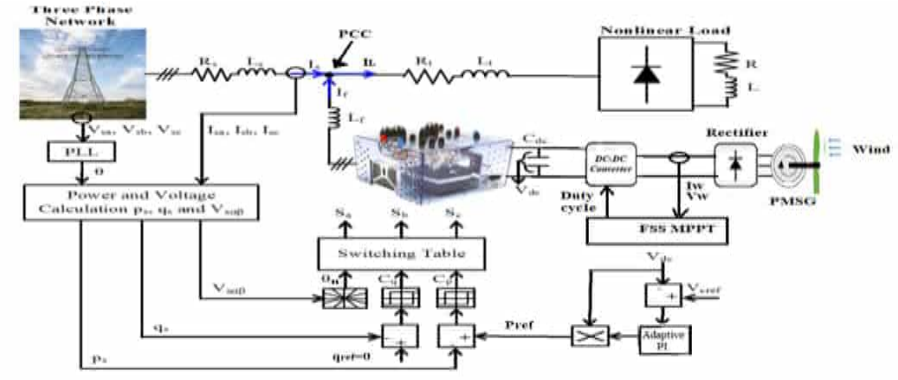

Figure 2: General control structure of the SAPF and the WECS.

after finding them. Once they have met their daily energy requirements, they begin looking for winter food sources (hickory nuts). Storing hickory nuts will help them meet their energy needs in difficult weather conditions, avoid costly foraging trips, and hence boost their chances of survival. Indeed, in the winter, the lack of leaf cover in deciduous woods increases the risk of predation, and as a result, they become less active but do not hibernate. As the winter season ends, flying squirrels become active again (Figure 3). This is a repetitive process that continues during a flying squirrel's foraging for food [11].

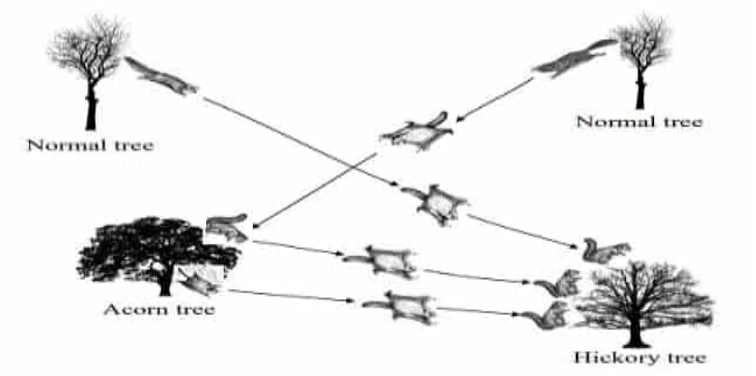

Figure 3: Flying Squirrel foraging habit.

3.1.2 FSSO algorithm steps for global maximum power point tracking

The power output of the WECS is used as the objective (food source) in MPPT, while the duty ratio 'd' of the boost converter is used as the decision variable (position).

To minimize the convergence time to global maximum power point (GMPP), the existing FSSO algorithm is modified with the elimination of the presence of predators. The various phases and processes of the FSSO algorithm to follow the GMPP are described as follows [12].

1. Initialization: Initially, the Nfs FS are positioned at different positions, which represent different values of the duty cycle of the boost converter in a limited duty cycle space solution :0< d_i < 0.5.

2. Fitness Assessment: The boost converter acts sequentially with each duty cycle (i.e., the position of each FS) in this step. The quality of the food source is determined by the instantaneous wind power $P_{wind}(d)$ for each duty cycle 'd'. This phase is performed for all duty cycles, and the MPPT objective fitness function is $f(d) = Max(P_{wind}(d))$.

3. Declaration and sorting: The hickory tree is declared to have the duty cycle with the maximum wind power output. The next best FS position is supposed to be on an acorn tree.The remaining FSs are presumed to be on normal trees.

4. Position update: The duty cycle update is performed after the seasonal monitoring condition has been verified. Duty cycles are updated using **(a)** if ($S_C^k < S_{min}$), other duty cycles are updated using **(b)**. Following that, the fitness is assessed.

(a). Seasonal monitoring condition: Introducing seasonal monitoring conditions ensures that the algorithm does not get stuck in the LMPP. The seasonal constant (S_C) and its minimum value (S_{min}) for a one-dimensional space are calculated as follows:

$$S_C^k = |d_{at}^k - d_{ht}|, \tag{1}$$

$$S_{min} = \frac{10e^{-6}}{(365)^{k/(k_m/2.5)}}, \tag{2}$$

where d_{ht} and d_{at} represent the squirrel position at the hickory and acorn trees, respectively; k is the current iteration number and k_m is the maximum number of iterations allowed. The duty ratios (FSs on normal trees) NTFS are relocated using the Lévy distribution for better search space exploration

$$d_{nt}^{k+1} = d_{nt}^k + s, \tag{3}$$

where d_{nt} represents the squirrel position at the normal tree and the step length s using the Lévy distribution is presented as

$$s \approx K\left(\frac{u}{|v|^{1/\beta}}\right)(d_{ht} - d_{nt}), \tag{4}$$

where the Lévy index β and step coefficient K are taken as 1.5 and 1.25, respectively, and u and v are determined from the normal distribution curve as

$$u \approx N(0, \sigma_u^2) \qquad v \approx N(0, \sigma_v^2) \tag{5}$$

if Γ denotes the integral gamma function, then the variables σ_u and σ_v are defined as

$$\sigma_u = \left(\frac{\Gamma(1+\beta)sin(\pi\beta/2)}{\Gamma\left(\frac{1+\beta}{2}\right)\beta(2)^{\left(\frac{\beta-1}{2}\right)}}\right)^{1/\beta} \qquad \text{and} \qquad \sigma_v = 1, \tag{6}$$

where $\Gamma(n) = (n-1)!$.

(b). Routine update: The squirrel on the hickory tree is not allowed to move. The squirrel on the acorn tree is making its way toward the hickory tree. Some squirrels from normal trees move toward the hickory tree, whereas the others move toward the acorn tree. The corresponding duty cycles are updated according to the following equations:

$$d_{at}^{k+1} = d_{at}^k + g_d G_c(d_{ht}^K - d_{at}^k), \tag{7}$$

$$d_{nt}^{k+1} = d_{nt}^{k} + g_d G_c (d_{ht}^{K} - d_{nt}^{k}), \tag{8}$$

$$d_{nt}^{k+1} = d_{nt}^{k} + g_d G_c (d_{at}^{K} - d_{nt}^{k}), \tag{9}$$

where G_c and g_d represent the gliding constant and gliding distance, respectively. The value of G_c is taken as 0.0019. The gliding distance g_d is expressed as

$$\begin{cases} g_d = \frac{h_g}{s_f tan\phi}, \\ \tan\phi = \frac{F_D}{F_L}, \end{cases} \tag{10}$$

where the value of the height loss after gliding (h_g) is taken to be $0.01m$; the scaling factor s_f is selected as 0.18. F_D and F_L are the drag and the lift forces, respectively, which are calculated as

$$\begin{cases} F_D = \frac{1}{2}\rho V^2 S C_D, \\ F_L = \frac{1}{2}\rho V^2 S C_L, \end{cases} \tag{11}$$

where ρ is the air density, V is the velocity of the squirrel, and S is the surface area of the body. The drag coefficient C_D is taken as 0.006 and the lift coefficient C_L is selected as 0.007.

5. Convergence determination: If the change in the position of all FSs is less than a threshold, or if the maximum number of iterations is achieved, the algorithm optimization is ended, and the duty cycle at which the boost converter works while tracking GMPP is selected as the output.

6. Re-initialization: The MPPT is a time variation optimization algorithm in which the fitness value varies with the weather. In such circumstances, the FSs positions (duty ratios) are re-initialized to look for the new GMPP. In this paper, the duty cycles are reinitialized after detecting the change in wind power through the following constraint equation:

$$\frac{P_{wind}^{k+1} - P_{wind}^{k}}{P_{wind}^{k+1}} \geq \Delta P(\%). \tag{12}$$

3.2 DC Link voltage PI controller tuned using sliding mode extremum seeking algorithm

The DC Link voltage controller is synthesized in this section. In the DC Link voltage control loop, the suggested adaptive PI controller is employed to reduce DC capacitor fluctuation voltages. As shown in Figure 4, the optimized PI controller is used to maintain the DC Link voltage at a specified value using the error between the measured DC Link voltage and its reference to control the output active power of the inverter. The proposed sliding-mode extremum seeking (SMES) technique is employed to adjust the parameters of the PI controller with the aim of minimizing a specified cost function [13, 14].

The block diagram for the overall control loop with the proposed sliding-mode extremum seeking PI controller is shown in Figure 4. The cost function is utilized to quantify the effectiveness of the PI controller.

In general, the Integrated Squared Error (ISE) is used as a cost function [13]:

$$J(\theta) = \frac{1}{T}\int_0^T [e(t,\theta)]^2 dt \tag{13}$$

and $\theta = [k_p \quad k_i]^T$ contains the PI parameters. The SMES algorithm updates the PI controller parameters θ to minimize the cost function $J(\theta)$.

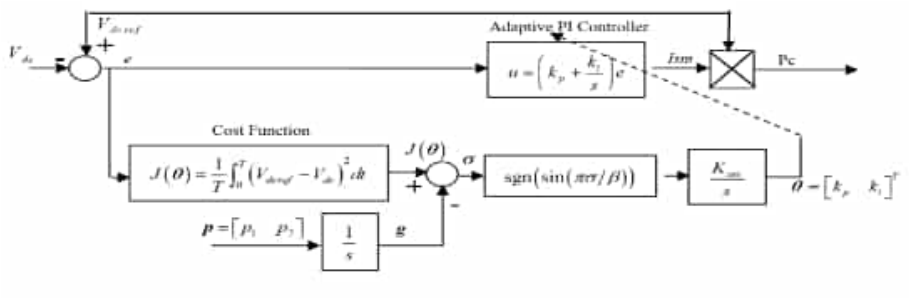

Figure 4: Block diagram for the overall control loop with the proposed multivariable sliding-mode extremum seeking PI controller.

The proposed sliding-mode extremum seeking algorithm applies two switching functions

$$\sigma = [\sigma_1 \quad \sigma_2] \tag{14}$$

to determinate the gains k_p and k_i of the PI controller. Each switching function is defined as

$$\sigma_i = J(\theta)) - p_i t, \tag{15}$$

$p_i > 0$ (i = 1, 2) represents the slope of the i-th sliding surface. The vector of driving signals is determined as

$$\mathbf{p} = [p_1 \quad p_2]. \tag{16}$$

According to Figure 4, g_i is an increasing reference function defined as $\dot{g}_i = p_i$. The parameter θ_i is considered as the optimal control law. It is designed to satisfy

$$\dot{\theta} = K_{ses_i} sgn(sin(\pi\sigma_i/\beta_i), \tag{17}$$

where K_{ses_i} and β_i are positive.

The proposed scheme adopts a minimal search method with a periodic switching function since the performance function is not known. This technique adapts the parameters of the PI controller to achieve the minimum point of the cost function and this by forcing the function $J(\theta)$ to rest on the increasing sliding surface vector.

4 Simulations Results

A MATLAB/Simulink model merging SAPF and WECS has been developed to validate the suggested control strategies under non-linear load conditions and wind speed variation.

We have adressed two cases: with and without the WECS. The WECS is not connected in the first case. Figure 5 depicts the source voltages, source current I_{as}, filter current I_{af}, and load current I_{aL} before and after SAPF compensation.

The source voltage waveform is sinusoidal and balanced, as seen in Figure 5. Before filtering, the source current waveform was distorted, but once the active filter was applied to the configuration (t = 0.25 s), the waveform immediately became sinusoidal.

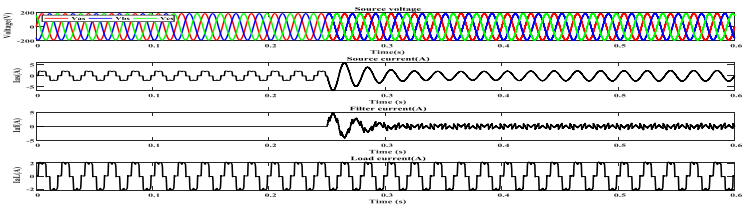

Figure 5: Source voltages, the source current I_{as}, the filter current I_{af}, and the load current I_{aL} before and after compensation by the shunt APF.

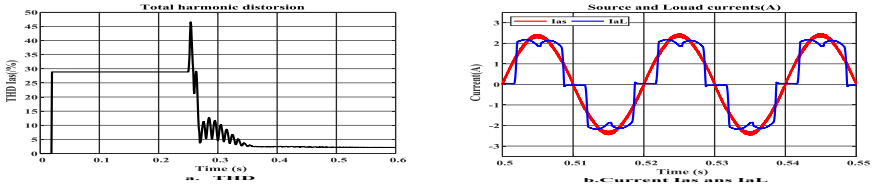

Figure 6: a. Temporal pattern of the THD without and with SAPF of the source current I_{as}. b. Source current I_{as}, and the load current I_{aL} with SAPF.

As shown in Figure 6a, the THD (Total Harmonic Distortion) decreases significantly after activating the filter on the electrical network, confirming the high quality of the filtering. Figure 6b shows that the source current meets the load requirement (I_{aL}).

In the second case, the WECS is connected to the shunt active power filter. We employed two wind speed profiles for the wind turbine, one at 5 m/s and the other at 9m/s. For both wind speed profiles, the form of the source current is clearly sinusoidal (Figure 7).

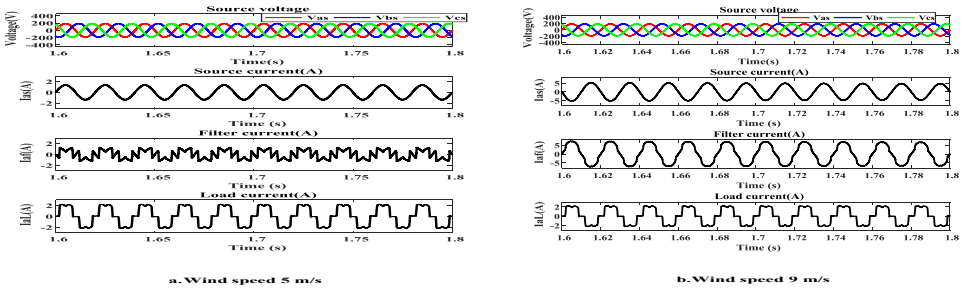

Figure 7: The source voltages, the source current I_{as}, the filter current I_{af}, and the load current I_{aL} for both wind speed.

According to Figure 8a, the charging current is supplied by the two sources (WECS and network); however, as illustrated in Figure 8b, part of the wind energy satisfies the load demand and the additional energy is injected into the power grid, which is justified

by the fact that there is a phase π between V_{as} and I_{as} (Figure 8b). In addition, the THD (Total Harmonic Distortion) complies with IEEE 519 standard, as seen in Figure 9.

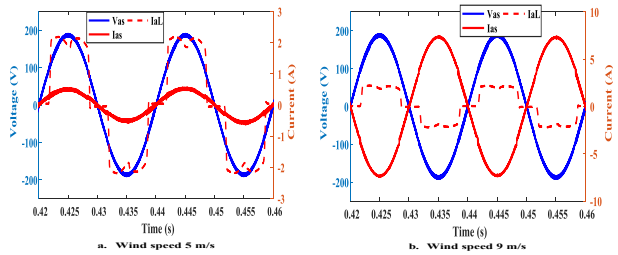

Figure 8: The source current I_{as} and the load current I_{aL} for both wind speeds.

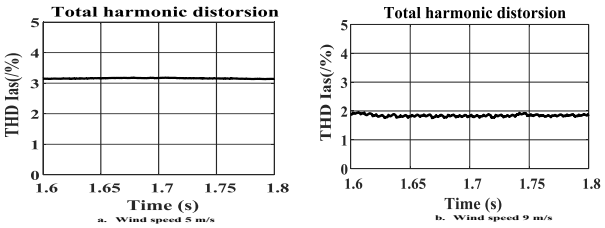

Figure 9: Temporal pattern of the THD for both wind speeds.

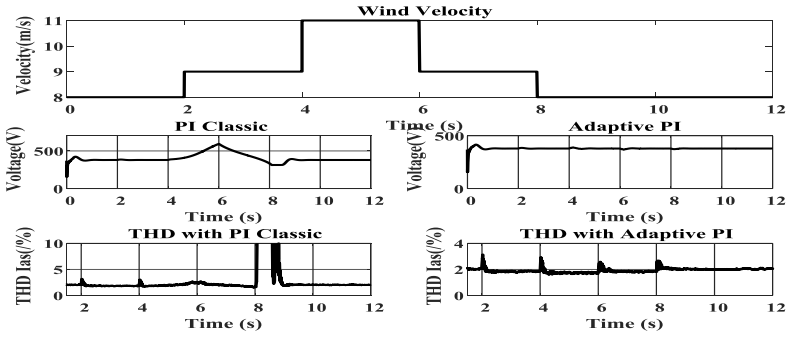

Figure 10: Dynamic performance of the classic DC Link PI controller and the adaptive PI controller with their associated THD.

As demonstrated in Figure 10, the adaptive PI controller considerably improves the dynamic performance of the DC Link voltage regulator as well as the THD of the source currents.

5 Conclusion

This paper focuses on the application of two regulators to control an active shunt power filter in order to improve the compensation of current harmonics injected by nonlinear charges. The first is an MPPT controller based on the flying squirrel search algorithm. The advantage of the proposed method is that it requires only the instantaneous current and voltage generated by the wind turbine to generate the duty cycle of the boost controller. The second regulator is an adaptive PI controller based on the sliding mode extreme search technique. It is used to control the dynamic performance of the DC Link voltage regulator. The proposed optimizer modifies the PI gains by minimizing a cost function based on the feedback error term. The resulting PI controller can exhibit fast and accurate tracking response as well as excellent disturbance rejection. The two proposed controllers are considered model-free algorithms. The three-phase inverter of the SAPS is controlled using a Direct Power Control (DPC) technique. According to the simulation results, the proposed system works efficiently. Indeed, the combination of the proposed control strategies makes it possible to reduce current harmonics according to the standard recommendations of the electrical energy quality (IEEE519) while injecting all the available power of the PMSG into the load and, in certain cases, into the power grid, particularly when the wind speed increases.

References

[1] M. Morsli, A. Tlemcani, A. Krama, A. Abbad L. Zellouma and H. Nouri. Application of the Direct Power Control Strategy in a Shunt Active Filter by Exploiting the Solar Photovoltaic Energy as a Continuous Source. *Nonlinear Dynamics and Systems Theory* **20** (4) (2020) 410–424.

[2] H. Wayne Beaty, M. F. McGranaghan, R. C. Dugan and S. Santoso. *Electrical Power Systems Quality, Second Edition*. McGraw-Hill, New York, 2008.

[3] M. Morsli, A. Tlemcani and M. S. Boucherit. Shunt Active Power Filter Based Harmonics Compensation of a Low-Voltage Network Using Fuzzy Logic System. *Nonlinear Dynamics and Systems Theory* **17** (1) (2017) 70–85.

[4] N. Mesbahi, A. Ouari, D. Ouldabdeslam, T. Djamah and A. Omeiri. Direct power control of shunt active filter using high selectivity filter (HSF) under distorted or unbalanced conditions. *Electric Power Systems Research* **108** (2014) 113–123.

[5] T. Trivedi, R. Jadeja and P. Bhatt. Improved direct power control of shunt active power filter with minimum reactive power variation and minimum apparent power variation approaches. *Journal of Electrical Engineering & Technology* **12** (3) (2017) 1124–1136.

[6] Juan Zhou, Yalei Yuan and Hao Dong. Adaptive DC-Link Voltage Control for Shunt Active Power Filters Based on Model Predictive Control. *IEEE Access* **8** (2020) 208348–208357.

[7] H. Gaied, M. Naoui, H. Kraiem, B. Srikanth Goud, A. Flah, L. M. L. Alghaythi, H. Kotb, S. G. Ali and K. Aboras. Comparative analysis of MPPT techniques for enhancing a wind energy conversion system. *Frontiers in Energy Research* (2022) 1–15.

[8] L. Xuan Chau M. Quan Duong and K. Hung Le. Review of the Modern Maximum Power Tracking Algorithms for Permanent Magnet Synchronous Generator of Wind Power Conversion Systems. *Energies* **16** (1) (2023) 1–25.

[9] M. H. Zafar, N. Mujeeb Khan, A. Feroz Mirza and M. Mansoor. Bio-inspired optimization algorithms based maximum power point tracking technique for photovoltaic systems under partial shading and complex partial shading conditions. *Journal of Cleaner Production* **309** 127279 (2021) 1–18.

[10] F. Hamidia and A. Abbadi. SOFC-PV System with Storage Battery Basedon Cuckoo Search Algorithm. *Nonlinear Dynamics and Systems Theory* **22** (4) (2022) 367–378.

[11] Y. Wang and T. Du. An Improved Squirrel Search Algorithm for Global Function Optimization. *Algorithms* **12** (80) (2019) 1–29.

[12] N. Singh, K. K. Gupta, S. K. Jain, N. K. Dewangan and P. Bhatnagar. A Flying Squirrel Search Optimization for MPPT Under Partial Shaded Photovoltaic System. *EEE Journal of Emerging and Selected Topics in Power Electronics* **9** (4) (2021) 4963–4978.

[13] T. Roux–Oliveira, L. R. Costa, A. V. Pino and P. Paz. Extremum Seeking-based Adaptive PID Control applied to Neuromuscular Electrical Stimulationl. *Anais da Academia Brasileira de Ciencias* **91** (1) (2019) 1–20.

[14] N. J. Killingsworth and M. Krstic. PID tuning using extremum seeking: online, model-free performance optimization. *IEEE Control Systems Magazine* **26** (1) (2006) 70–79.